Synthetic Metals xxx (2010) xxx–xxx

Contents lists available at ScienceDirect

Synthetic Metals

journal homepage: www.elsevier.com/locate/synmet

n- and p-Channel field-effect transistors based on diquinoxalinoTTF derivatives

Naraso Borjigin[a,c,*,1], Jun-ichi Nishida[a], Shizuo Tokito[b], Luke Theogarajan[c], Yoshiro Yamashita[a]

[a] Department of Electronic Chemistry, Interdisciplinary Graduate School of Science and Engineering, Tokyo Institute of Technology, Nagatsuta, Midori-ku, Yokohama 226-850 Japan
[b] NHK Science and Technical Research Laboratories, Kinuta, Setagaya-ku, Tokyo 157-851, Japan
[c] California NanoSystems Institute (CNSI), University of California, Santa Barbara, CA 93106-6105, United States

ARTICLE INFO

Article history:
Received 6 July 2010
Received in revised form 2 September 2010
Accepted 4 September 2010
Available online xxx

Keywords:
TTF
Tetrathiafulvalene
Electron withdrawing
Electron donating
HOMO
LUMO
n-type FET
p-type FET
Field-effect transistor

ABSTRACT

Three new quinoxalinoTTF derivatives with methyl, trifluoromethyl and fluoro groups were synthesized and characterized by UV–vis absorption spectroscopy, differential scanning calorimetry, X-ray single crystal analysis, X-ray diffraction, and field-effect transistor (FET) characteristics. All of them have π-stacking structures in the single crystals. The quinoxalinoTTF derivative with trifluoromethyl groups exhibited an n-type FET, which is a rare example of n-channel FETs based on TTF derivatives. The highest electron mobility is 0.01 $cm^2 V^{-1}$ s. The FET polarity was converted to p-channel from n-channel by replacing the trifluoromethyl groups with methyl groups. The hole mobility is as high as 0.2 $cm^2 V^{-1}$ s. In contrast, the fluoro substituted derivative did not show FET properties due to the poorly ordered molecular arrangement.

1. Introduction

Organic field-effect transistors (OFETs) [1] have drawn great interest in recent years due to their potential applications in low-cost, large-area and flexible electronics, such as electronic papers and flexible displays [2]. The performance of OFET devices is influenced by several factors such as the HOMO–LUMO energy levels of the material, molecular orientations on the substrate, solid-state properties and thin-film stability. OFETs based on oligothiophenes and oligoacenes have been intensively studied during the past two decades [3]. The development of new materials is particularly important for the progress of this field. Recently, tetrathiafulvalene (TTF) derivatives were reported to exhibit excellent FET performance as single crystals [4]. However, their thin films are sensitive to oxygen, resulting in poor FET performances [5]. We introduced aromatic fused benzene rings and nitrogen heterocycles to the TTF skeleton and the compounds exhibited excellent FET properties as thin films [6a]. The motivation for introducing fused aromatic rings was to decrease the strong electron-donating ability of TTF derivatives and also enhance their air stability. A high hole mobility of 0.42 $cm^2 V^{-1} s^{-1}$ was observed with dinaphthoTTF (DN-TTF). Even more recently, we introduced electron-withdrawing halogen groups to diquinoxalinoTTF (DQ-TTF) and succeeded in preparing n-type FETs based on TTF derivatives for the first time [6b]. Compared to p-type semiconductors, the number of n-type semiconductors is still limited, and their FET performances are not satisfactory [7]. The development of good n-type materials is crucial for the fabrication of p–n junctions, bipolar transistors, and integrated circuits [8]. To obtain high electron mobility, organic semiconductors should have proper LUMO energy levels near the work function of the electrodes. High performance n-type organic semiconductors have recently been obtained by introducing electron-withdrawing trifluoromethyl groups into electron-donating heterocyclic oligomer systems [9]. Therefore, we have now introduced trifluoromethyl groups to the TTF derivative and succeeded in obtaining n-type FETs. In contrast to the n-channel tetrahalogen derivatives previously reported, the trifluoromethyl substituted derivative has better solubility in common organic solvents. We also introduced methyl groups to the DQ-TTF core to obtain a p-channel high mobility material. On the other hand, a diflouro substituted derivative did not exhibit FET characteristics since the disordered fluorine end groups result in unfavorable morphology in the thin film.

* Corresponding author at: California NanoSystems Institute (CNSI), University of California, Elings Hall, Room 2411, Santa Barbara, CA 93106-6105, United States. Tel.: +1 805 637 1103.
E-mail address: narsobr@yahoo.com (N. Borjigin).
[1] The author's name was used as Naraso in previous publications [6].

0379-6779/$ – see front matter © 2010 Elsevier B.V. All rights reserved.
doi:10.1016/j.synthmet.2010.09.005

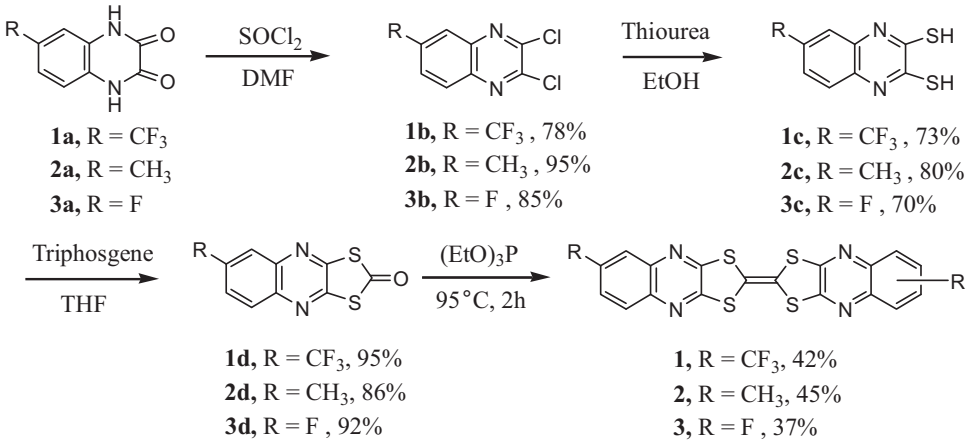

Scheme 1. Synthesis of TTF derivatives.

2. Results and discussion

2.1. Synthesis and characterization

New TTF derivatives **1**–**3** were synthesized by a phosphite homo coupling reaction as shown in Scheme 1. The 1,4-dihydroquinoxaline-2,3-diones were converted to their corresponding dichloro compounds by treatment with thionyl chloride in a small amount of DMF. The dichloroquinoxalines were then refluxed with thiourea in ethanol for 2 h. The solvent was removed under reduced pressure, and an NaOH solution was added to decompose the intermediate salt. Acidification with acetic acid afforded the quinoxaline-2,3-dithiols (see Supporting information). The corresponding thiols were dissolved in THF (anhyd), triphosgene was added, and the mixtures were stirred for 3 h at rt to give the ketones. The ketones then were heated in triethyl phosphite at 95 °C for 2 h in an oil-bath. The resulting red solid was filtered off, washed with dichloromethane and sublimed to give these TTF derivatives. The structures were characterized by mass spectrometry and elemental analysis. The thermal properties of these derivatives were investigated by differential scanning calorimetry (DSC) measurements. The melting points of TTF derivatives **1**–**3** were higher than 400 °C, indicative of the high-thermal stability and the existence of strong intermolecular interactions in the solid state.

2.2. Electrochemical properties

The absorption spectra (Fig. 1) show that DQ-TTF and **1** have absorption maxima at around 450 nm. On the other hand, the trifluoromethyl TTF derivative **2** has an absorption maximum at 462 nm due to the effect of the stronger electron-withdrawing group. The electrochemical property of **3** could not be measured due to the low solubility.

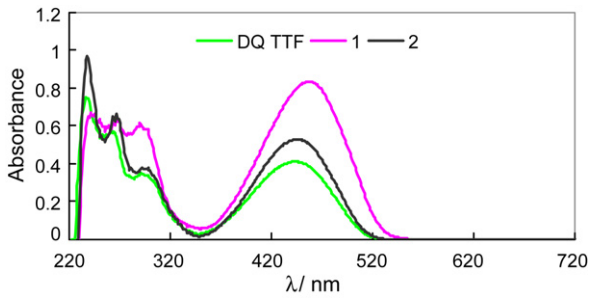

Fig. 1. UV–vis spectra of TTF derivatives DQ-TTF, **1** and **2** in CH_2Cl_2.

Utilizing the differential pulse voltammetry (DPV), the first oxidation potentials were measured at 1.12 V, 1.08 V and 1.28 V for DQ-TTF, **1** and **2**, respectively (see Supporting information). The methyl derivative has a lower oxidation potential due to the effect of the two electron-donating methyl groups. On the other hand, the trifluoromethyl compound exhibited the highest oxidation potential due to the effect of two electron-withdrawing trifluoromethyl groups. The reduction potentials were not observed in these TTF derivatives in the available DPV measurement range of CH_2Cl_2.

2.3. Single crystal structures

Single crystals of **1**, **2** and **3** suitable for structural analysis were obtained by slow sublimation. These molecules are completely planar and exhibit face-to-face π-stacking as shown in Fig. 2. In the

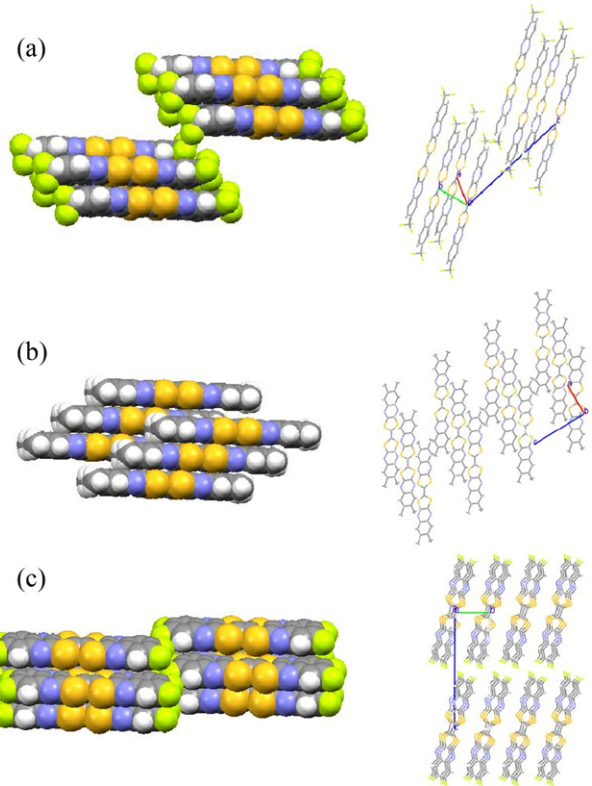

Fig. 2. π-Stacking and molecular arrangement, (a) for **1**, (b) for **2** and (c) for **3**.

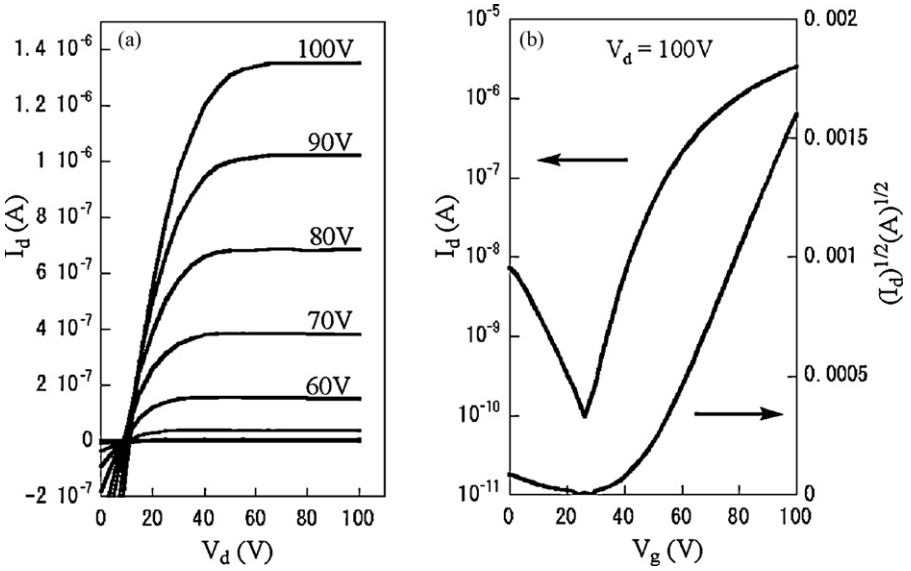

Fig. 3. Drain-source current (I_{ds}) versus drain-source voltage (V_{ds}) characteristics, I_d and $I_d^{1/2}$ versus V_g plots for **1**.

crystal structure of **1**, the 1,3-dithiole rings are overlapped with the pyrazine rings, suggesting the presence of intermolecular charge-transfer interactions between the donor and acceptor moieties. Only the trans isomer was observed in the X-ray crystal structure of **1**, where the interplanar distance is 3.34 Å. The 1,3-dithiole rings are also overlapped with the pyrazine rings in this molecule and an intermolecular short S···S contact of 3.66 Å is observed between the neighboring molecules (Fig. 2(a)). The similar π-stacking was observed in the crystal structures of **2** (Fig. 2(b)). However, both the cis and trans isomers were present as 9:11ratio in this structure, where the interplanar distance is 3.43 Å. The cis–trans ratio was determined by the lowest R-factor in the crystallography. On the other hand, in the crystal structure of **3**, the cis–trans ratio is also 2:3, where the fluoro substituents form hydrogen bonds (2.50 Å) with the neighboring H substituent along with the *c*-axis. This hydrogen bond network may force the donor–acceptor units of the TTF derivative to overlap in a segregated manner, resulting in a lack of intermolecular charge transfer in the single crystal of difluoro derivative **3** in contrast to **1** and **2**.

2.4. Field-effect transistors

Top contact configurations were used to make the FET devices. The n-doped silicon substrate was used as the gate. The gold electrodes were defined after semiconductor deposition by using shadow masks with *W*/*L* of 1.0 mm/100 μm and 1.0 mm/50 μm. The SiO_2 gate dielectric was 200 nm thick. The electrical characteristics were obtained at room temperature under ultra high vacuum conditions using a semiconductor parameter analyzer (Figs. 3 and 4).

The FET performances are summarized in Table 1. The derivative **1** showed high electron mobility and high on/off ratio, which is currently the third example of n-type FETs using TTF derivatives. Fig. 3 shows the drain current (I_d) versus voltage (V_d) characteristics for the FET devices of **1**, where the electron mobilities calculated in the saturation regime were at the range of 0.005–0.01 $cm^2\ V^{-1}\ s^{-1}$. In contrast, the methyl derivative **2** exhibited p-type performance with the hole mobilities of 0.1–0.2 $cm^2\ V^{-1}\ s^{-1}$. However, the flouro derivative **3** did not exhibit the FET properties.

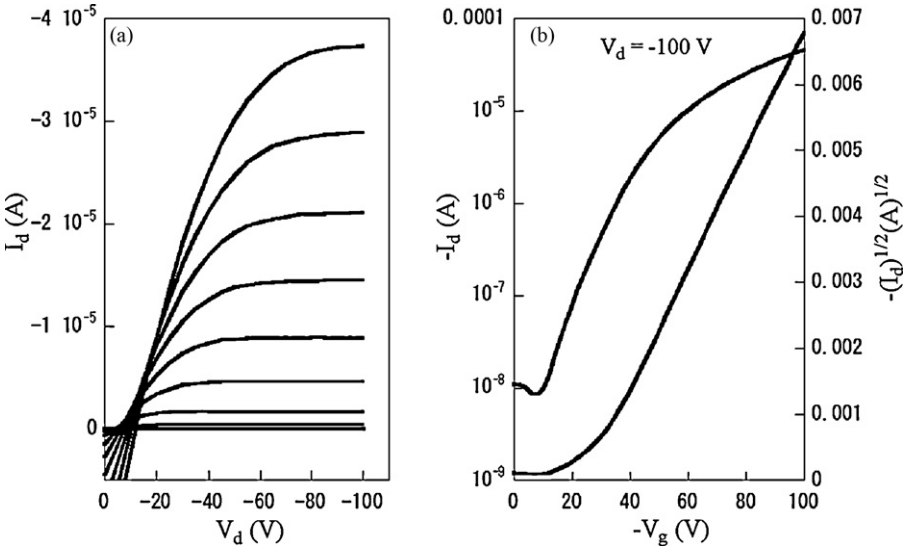

Fig. 4. Drain-source current (I_{ds}) versus drain-source voltage (V_{ds}) characteristics, I_d and $I_d^{1/2}$ versus V_g plots for **2**.

Please cite this article in press as: N. Borjigin, et al., Synthetic Met. (2010), doi:10.1016/j.synthmet.2010.09.005

Table 1
Orbital energies and FET characteristics of these TTF derivatives.

Compounds	HOMO (eV)[b]	LUMO (eV)[d]	Mobility ($cm^2 V^{-1} s^{-1}$)	On/off ratio	V_{th} (V)
DQ-TTF (p-Type)[a]	−5.38	−3.27	0.20	10^6	−36
1 (n-Type)	−5.68	−3.64	0.01	10^4	44
2 (p-Type)	−5.32	−2.99	0.20	2.3×10^4	−24
3[c]	No gate effect				

[a] Ref. [6a].
[b] Calculated from oxidation potentials, ferrocene used as internal standard.
[c] The oxidation potentials were not obtained, due to the low solubility.
[d] Estimated from the HOMO and optical energy gaps.

2.5. Film structures

To investigate the relationship between the film structures and FET performances, the films of TTF derivatives **1**–**3** deposited on the SiO_2/Si substrate at room temperature were evaluated by X-ray diffraction in reflection mode (XRD). Fig. 5(a)–(c) shows clear X-ray diffraction patterns of films of **1**, **2** and **3**. In the thin film of **1**, sharp reflections up to the sixth order are observed. The strong intensity of the X-ray diffraction peaks indicates the formation of lamellar ordering and crystallinity on the substrate. The *d*-spacing of **1** obtained from the first reflection peak is 1.81 nm, comparable to the molecular length obtained from the single crystal X-ray analysis (1.83 nm), suggesting that the molecules stand perpendicularly to the substrate. For the thin film of **2**, the *d*-spacing obtained from the first reflection peak is 1.61 nm. Since the molecular length obtained from the single crystal X-ray analysis is 1.88 nm, the molecules are considered to have a ca. 31 declining orientation on the substrate. The thin film of **3** has two primary peaks, the *d*-spacing of 1.82 nm of the first peak is almost identical to the layer spacing of 1.86 nm along the *c*-axis in the single crystal, the second primary peak (*d*-space of 0.53 nm) is identical to the layer spacing of 0.56 nm along the *b*-axis. This indicates that two kinds of morphologies exist in the thin-film state.

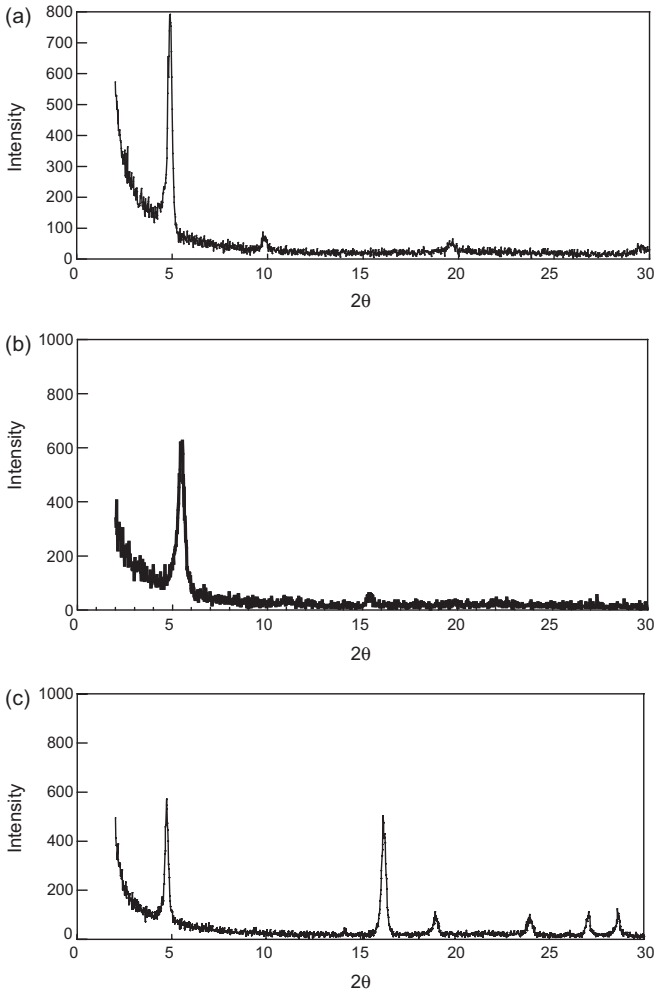

Fig. 5. X-ray diffraction of films (50-nm thickness) deposited at room temperature, (a) for 1, (b) for 2 and (c) for 3.

3. Conclusion

We have prepared a series of quinoxalinoTTF derivatives containing trifluoromethyl, methyl and fluoro groups. The introduction of electron-withdrawing or electron-donating groups to the TTF skeleton was effective to change the HOMO or LUMO energies, leading to good n- or p-type FET performances in the thin films. The films of trifluoromethyl derivative of **1** exhibited high electron mobility, which is the rare example of n-type FETs using a TTF derivative. On the other hand, the methyl substituted TTF derivative **2** exhibited p-type FET performances with high hole mobility. These compounds showed sharp XRD peaks, indicating the formation of lamellar ordering and crystallinity on the substrate. Moreover, these TTF derivatives have face-to-face π-stacking in the crystal structures, where short intermolecular S···S contacts were observed. The strong intermolecular interactions may lead to the high performance FET properties. On the other hand, the fluoro substituted derivative **3** did not show FET properties due to its two morphologies in the thin film as well as the weak intermolecular interaction in the solid state.

4. Experimental procedure

4.1. General information

Melting points were obtained on a Yanaco melting point apparatus and were uncorrected. EI mass spectra were collected on a JEOL JMS-700 mass spectrometer. UV–vis spectra were recorded on a SHIMADZU MultiSpec-1500. Differential pulse voltammograms were recorded on a BAS-100B system using terabutylammonium hexafluorophoshate ($TBAPF_6$) (0.1 mol dm^{-3} in dry dichloromethane). The Pt disk, Pt wire and SCE were used as working, counter, and reference electrodes, respectively. Elemental analyses were performed at the Tokyo Institute of Technology, Chemical Resources Laboratory.

4.2. Synthesis

4.2.1. 6-Trifluoromethyl-1,3-dithia-4, 9-diazacyclopenta[b]-naphthalen-2-one (**1d**)

6-Trifluoromethylquinoxaline-2,3-dithiol **1c** (0.75 g/2.86 mmol) was dissolved in 25 ml of THF (anhyd). Triphosgene (2 g/6.75 mmol) was added and stirred for 3 h to give 6-

trifluoromethyl-1,3-dithia-4,9-diaza-cyclopenta[b]naphthalen-2-one **1d** (0.78 g, 95%).

MS (EI): *m*/*z* (%) 288 (M^+, 100); mp 130–137 °C;

^{1}H-NMR (CDCl3; 300 MHz): δ7.62 (s, 1H), 7.74 (s, 1H), 8.07 (s, 1H).

*4.2.2. 6-Methyl-1,3-dithia-4,9-diazacyclopenta[b]naphthalen-2-one (**2d**)*

Yield 86%, MS (EI): *m*/*z* (%) 234 (M^+, 100); mp 133–140 °C;

^{1}H-NMR ($CDCl_3$; 300 MHz): δ7.36 (s, 1H), 7.34 (s, 1H), 7.07 (s, 1H), 2.05 (s, 3H).

*4.2.3. 6-Fluoro-1,3-dithia-4,9-diazacyclopenta[b]naphthalen-2-one (**3d**)*

Yield 92%, MS (EI): *m*/*z* (%) 280 (M^+, 100); mp 150–157 °C;

^{1}H-NMR ($CDCl_3$; 300 MHz): δ7.12 (s, 1H), 7.23 (s, 1H), 7.56 (s, 1H).

*4.2.4. 6,6′-Bistrifluoromethyl[2,2′]bi[1,3-dithia-4,9-diazacyclopenta[b]naphthalenylidene] (**1**)*

298 mg (0.20 mmol) of 6,7-dichloro-1,3-dithia-4,9-diazacyclopenta[b]naphthalen- 2-one was heated in triethyl phosphite (2 ml) at 95 °C for 2 h in an oil-bath. The resulting dark red solid was filtered off, and washed with hexane and dichloromethane. The solid was purified by sublimation to give **3** (0.03 g, 30%). Red solid (yield 42%) MS (EI): *m*/*z* (%) 544 (M^+, 100); mp. 440–447 °C.

Anal. Calcd. For $C_{20}H_6F_6N_4S_4$: C, 44.11; H, 1.11; F, 20.93; N, 10.29; S, 23.55.

Found: C, 44.40; H, 1.22; N, 10.22; S, 23.30.

*4.2.5. 6,6′-Dimethyl[2,2′]bi[1,3-dithia-4,9-diazacyclopenta[b]naphthalenylidene] (**2**)*

Red solid (yield 45%) MS (EI): *m*/*z* (%) 436 (M^+, 100); mp. 403–410 °C.

Anal. Calcd. For $C_{20}H_{12}N_4S_4$: C, 55.02; H, 2.77; N, 12.83; S, 29.38.

Found: C, 54.94; H, 2.43; N, 12.64; S, 29.64.

*4.2.6. 6,6′-Difluoro[2,2′]bi[1,3-dithia-4,9-diazacyclopenta[b]naphthalenylidene] (**3**)*

Red solid (yield 37%) MS (EI): *m*/*z* (%) 444 (M^+, 100); mp. 450–457 °C.

Anal. Calcd. For $C_{18}H_6F_2N_4S_4$: C, 48.63; H, 1.36; F, 8.55; N, 12.60; S, 28.85.

Found: C, 48.64; H, 1.36; N, 12.60; S, 28.73.

The single-crystal X-ray measurements of TTF derivatives **1**, **2** and **3** were carried out on a Rigaku RAXIS-RAPID Imaging Plate diffractometer (Mo Kα radiation, λ = 0.71075 Å). The data were collected at 93 K and the structures were solved by the direct method (SIR97) and expanded using Fourier techniques. Non-hydrogen atoms were refined anisotropically. Hydrogen atoms were placed in geometrically calculated positions.

1: crystal size: 0.30 mm × 0.20 mm × 0.05 mm. Triclinic, *P*1(#2), *Z* = 1. *a* = 4.848(5), *b* = 5.634(6), *c* = 17.97(3) Å, α = 87.93(5), β = 86.06(5), γ = 76.76(4), *V* = 476(3) Å^3, $2\theta_{max}$ = 55.1, ρ_{calcd} = 1.764 g/cm^3. Of 4279 reflections, 1985 were unique (R_{int} = 0.036), GOF = 1.20, R_1 = 0.051, R_w = 0.142 (for all reflections).

2: crystal size: 0.10 mm × 0.20 mm × 0.30 mm. Triclinic, *P*1(#2), *Z* = 1. *a* = 5.863(7), *b* = 7.46(1), *c* = 10.46(1) Å, α = 96.62(5), β = 90.12(4), γ = 97.97(5), *V* = 449(3) Å^3, $2\theta_{max}$ = 55.0, ρ_{calcd} = 1.612 g/cm^3. Of 4455 reflections, 2050 were unique (R_{int} = 0.014), GOF = 1.26, R_1 = 0.032, R_w = 0.096 (for all reflections).

3: crystal size: 0.30 mm × 0.30 mm × 0.10 mm. Triclinic, *P*1(#2), *Z* = 1. *a* = 3.790(4), *b* = 5.669(8), *c* = 18.68(2) Å, α = 90.19(4), β = 92.55(4), γ = 93.82(4), *V* = 400(2) Å^3, $2\theta_{max}$ = 55.0, ρ_{calcd} = 1.845 g/cm^3. Of 1811 reflections, 1533 were unique, GOF = 1.29, R_1 = 0.033, R_w = 0.0962 (for all reflections).

4.3. Fabrication of OFETs

OFETs were constructed on heavily doped n-type silicon wafers covered with 2000 Å-thick thermally grown silicon dioxide. The silicon dioxide acted as a gate dielectric layer, and the silicon wafer served as a gate electrode. Organic compounds were deposited on the silicon dioxide by vacuum evaporation at a rate of 0.2–0.3 Å s^{-1} under pressure of 10^{-5} Pa. The thickness of the semiconductor layer was 500 Å. During the evaporation, the temperature of the substrate was maintained by heating a copper block on which the substrate was mounted. Gold was used as the source and drain electrodes and was deposited on the organic semiconductor layer through a shadow mask with a channel width (*W*) of 1000 μm and a channel length (*L*) of 100, 75 and 50 μm. Finally, the FET measurements were carried out at room temperature in the vacuum chamber (10^{-5} Pa) without exposure to air with the Hewlett-Packard 4140A and 4140B models.

4.4. X-ray diffraction studies

X-ray diffraction (XRD) measurements were carried out with a JEOL JDX-3530 X-ray diffractometer system. XRD patterns were obtained using Bragg-Brentano geometry with Cu Kα radiation as the X-ray source with an acceleration voltage of 40 kV and a beam current of 30 mA.

Appendix A. Supplementary data

Supplementary data associated with this article can be found, in the online version, at doi:10.1016/j.synthmet.2010.09.005.

References

[1] (a) H.E. Katz, Z. Bao, S.L. Gilat, Acc. Chem. Res. 34 (2001) 359;
(b) A. Facchetti, M.-H. Yoon, C.L. Stern, H.E. Katz, T. Marks, J. Angew. Chem. Int. Ed. 42 (2003) 3900;
(c) C.D. Dimitrakopoulos, P.R.L. Malenfant, Adv. Mater. 14 (2002) 99;
(d) H. Moon, R. Zeis, E.J. Borkent, C. Besnard, A.J. Lovinger, T. Siegrist, C. Kloc, Z. Bao, J. Am. Chem. Soc. 126 (2004) 15322.
[2] (a) A. Facchetti, M. Mushrush, H.E. Katz, T. Marks, J. Adv. Mater. 15 (2003) 33;
(b) A. Facchetti, J. Letizia, M.-H. Yoon, M. Mushrush, H.E. Katz, T. Marks, J. Chem. Mater. 16 (2004) 4715;
(c) K. Takimiya, Y. Kunugi, Y. Konda, H. Ebata, Y. Toyoshima, T. Otsubo, J. Am. Chem. Soc. 128 (2006) 3044.
[3] (a) A. Afzali, C.D. Dimitrakopoulos, T.L. Breen, J. Am. Chem. Soc. 124 (2002) 8812;
(b) M.M. Payne, S.R. Parkin, J.E. Anthony, C.-C. Kuo, T.N. Jackson, J. Am. Chem. Soc. 127 (2005) 4986;
(c) G.S. Tulevski, Q. Miao, A. Afzali, T.O. Graham, C.R. Kagan, C. Nuckolls, J. Am. Chem. Soc. 128 (2006) 1788.
[4] (a) M. Mas-Torrent, M. Durkut, P. Hadley, X. Ribas, C. Rovira, J. Am. Chem. Soc. 126 (2004) 984;
(b) M. Mas-Torrent, P. Hadley, S.T. Bromley, N. Crivillers, J. Veciana, C. Rovira, Appl. Phys. Lett. 86 (2005) 012110.
[5] (a) B. Noda, M. Katsuhara, I. Aoyagi, T. Mori, T. Taguchi, T. Kambayashi, K. Ishikawa, H. Takezoe, Chem. Lett. 34 (2005) 392;
(b) M. Katsuhara, I. Aoyagi, H. Nakajima, T. Mori, T. Kambayashi, M. Ofuji, Y. Takanishi, K. Ishikawa, H. Takezoe, H. Hosono, Synth. Met. 149 (2005) 219.
[6] (a) Naraso, J. Nishida, S. Ando, J. Yamaguchi, K. Itaka, H. Koinuma, H. Tada, S. Tokito, Y. Yamashita, J. Am. Chem. Soc. 127 (2005) 10142;
(b) Naraso, J. Nishida, D. Kumaki, S. Tokito, Y.J. Yamashita, Am. Chem. Soc. 128 (2006) 9598;
(c) Naraso, J. Nishida, M. Tomura, Y. Yamashita, Synth. Met. 153 (2005) 389;
(d) Naraso, J. Nishida, D. Kumaki, S. Tokito, Y. Yamashita, Asian Chem. Lett. 11 (2007) 179.
[7] (a) M. Mushrush, A. Facchetti, M. Lefenfeld, H.E. Katz, T. Marks, J, J. Am. Chem. Soc. 125 (2003) 9414;
(b) H. Klauk, M. Halik, U. Zschieschang, F. Eder, G. Schmid, C. Dehm, Appl. Phys. Lett. 82 (2003) 4175;
(c) H.E. Katz, X.M. Hong, A. Dodabalapur, R.J. Sarpeshkar, Appl. Phys. 91 (2002) 1572.
[8] (a) Y. Sakamoto, T. Suzuki, M. Kobayashi, Y. Gao, Y. Fukai, Y. Inoue, F. Sato, S.J. Tokito, Am. Chem. Soc. 126 (2004) 8138;

(b) M.-H. Yoon, S.A. DiBenedetto, A. Facchetti, T.J.J. Marks, Am. Chem. Soc. 127 (2005) 1348;
(c) C.R. Newman, C.D. Frisbie, D.A. da Silva Filho, J.-L. Breĭdas, P.C. Ewbank, K.R. Mann, Chem. Mater. 16 (2004) 4436.
[9] (a) A. Facchetti, Y. Deng, A. Wang, Y. Koide, H. Sirringhaus, T.J. Marks, R.H. Friend, Angew. Chem. Int. Ed. 39 (2000) 4547; (b) J.A. Letizia, A. Facchetti, C.L. Stern, M.A. Ratner, T.J. Marks, J. Am. Chem. Soc. 127 (2005) 13476;
(c) S. Ando, R. Murakami, J. Nishida, H. Tada, Y. Inoue, S. Tokito, Y. Yamashita, J. Am. Chem. Soc. 127 (2005) 14996;
(d) A. Bolag, M. Mamada, J. Nishida, Y. Yamashita, Chem. Mater. 21 (2009) 4450.

Please cite this article in press as: N. Borjigin, et al., Synthetic Met. (2010), doi:10.1016/j.synthmet.2010.09.005